Angle-resolved-photoemission study of the $BaPb_{0.81}Bi_{0.19}O_3$ (001) surface

W. R. Flavell, M. Mian, and B. C. Morris
Department of Chemistry, The University of Manchester Institute of Science and Technology, P.O. Box 88, Manchester M60 1QD, United Kingdom

P. L. Wincott
Interdisciplinary Research Centre in Surface Science and Department of Chemistry, University of Manchester, Manchester M13 9PL, United Kingdom

D. Teehan and D. S-L. Law
Science and Engineering Research Council Daresbury Laboratory, Daresbury, Warrington, Cheshire WA4 4AD, United Kingdom

(Received 19 August 1993)

Synchrotron-excited angle-resolved photoemission data for a cleaved single-crystal $BaPb_{0.81}Bi_{0.19}O_3$ (001) surface are presented. Enhancements in spectral intensity at the Fermi energy away from the Γ point are shown to be in reasonable agreement with linear-augmented-plane-wave band-structure calculations [Phys. Rev. B **28**, 4227 (1983)]. The rapid surface degradation of metallic and superconducting compositions in the $BaPb_{1-x}Bi_xO_3$ system is discussed.

The perovskite $BaPb_{1-x}Bi_xO_3$ is a high-temperature superconductor in the composition range $0.05 \leq x \leq 0.3$, with a maximum T_c of around 13 K at $x = 0.25$.[2] The material undergoes a charge-density-wave- (CDW-) driven transition to a semiconducting state at $x \approx 0.4$.[3] Unlike the well-studied cuprate materials, the Bi systems are the only high-temperature oxide superconductors to show fully three-dimensional conductivity, leading to speculation that the mechanism of electron pairing in the superconducting phase may differ in the two types of material. It has been suggested that charge-density waves may provide that attractive interaction in doped $BaBiO_3$, by analogy with proposed mechanisms involving spin-density waves in the copper-oxide superconductors.[4] However, despite considerable theoretical interest in this system, it has been comparatively little studied by photoemission[5-13] and a number of fundamental features remain unresolved. In particular, there have been few reports of valence-band photoemission from single crystals of the doped material,[5,7,9] and, to the best of our knowledge, no angle-resolved band mapping measurements on such materials have been reported. Possible reasons for this paucity of data include difficulties in growing and satisfactorily cleaving large single crystals of the material and the marked instability of freshly prepared surfaces of metallic compositions to degradation in UHV.[5,7,13,14] The difficulties associated with producing clean, stable, and representative surfaces of this material[5,7,13,14] and associated materials such as $Ba_{1-x}K_xBiO_3$ (Ref. 15) have been noted in the literature.

Here we present angle-resolved valence-band photoemission data from a single-crystal sample of metallic and superconducting $BaPb_{0.81}Bi_{0.19}O_3$ (001), where degradation over the time period of the experiment has been minimized by cleaving a high-quality single-crystal sample held close to liquid-nitrogen temperature.[5,7] The nature of the degradation is discussed.

Angle-resolved-photoemission measurements employed the toroidal grating monochromator ($15 \leq h\nu \leq 90$ eV), VG ADES 400 instrument and low-temperature manipulator on station 6.2 at the Synchrotron Radiation Source, Daresbury Laboratory. The combined (monochromator and analyzer) energy resolution was 0.15 eV, and an analyzer entrance aperture was used to fix the angular resolution at $\pm 2°$ (FWHM). A single-crystal sample of $BaPb_{0.81}Bi_{0.19}O_3$, grown from a molten BaO-PbO-PbO_2-Bi_2O_3 solution[16] was provided by the UK National Crystal Growth Centre for Superconducting Oxides. The quoted Bi:Pb ratio was determined by EPMA, and the crystal showed a superconducting transition temperature, T_c, of 7 K; as expected, this is slightly below T_c(max) of 13 K observed at around $x = 0.25$. A large ($\approx 10 \times 5$ mm^2) single face of the crystal was shown by x-ray diffraction and Laue back reflection to be of (001) orientation. The lattice parameters derived from x-ray diffraction were used, together with the established Vegard's relationship for this phase,[17,18] to determine the bulk Pb:Bi ratio. This was found to be 0.8:0.2, entirely consistent with the result from EPMA. The crystal was cleaved in UHV in a direction parallel to this large (001) face using a VSW crystal cleaving anvil. During the cleaving process and subsequent data accumulation, the sample was held close to liquid-nitrogen temperature. The base pressure of the spectrometer was maintained at $\approx 3 \times 10^{-10}$ mbar. Sample cleanliness was monitored using a phi double-pass CMA to measure Auger spectra, and using the valence-band photoemission, particularly in the region of 9-eV binding energy, where a new feature is seen to appear in the spectrum as the surface degrades.[5,13] The problems of rapid degradation of metallic compositions in this system have been well documented by ourselves[13,14] and others.[5] In this respect, the cleaved crystal held at low temperature proved to be more stable than, for example, scraped ceramic samples.[13] Data accumulation was possible for several hours before significant degradation occurred. Following removal

from the spectrometer, Laue back reflection from the cleaved surface confirmed the (001) orientation. Some slight splitting of the diffracted beams was observed. Assuming the material to be orthorhombic (if only partially, see below) (Refs. 3 and 17) or monoclinic[19] at this composition, this was interpreted as evidence of *ab* twinning from a comparison between measured patterns and those calculated using NEWLAUE software (part of the LAUE suite available at the Daresbury Laboratory). In fact, the exact symmetry of the phase in the superconducting regime remains a matter of considerable controversy;[18] this is discussed further below.

Figure 1(a) shows angle-resolved valence-band spectra from the crystal, recorded at 33-eV photon energy. Vertical (ϕ) and horizontal (θ) analyzer positions with respect to the experimental (chamber) axes are shown. Unfortunately, problems associated with mounting the crystal meant that the experimental and crystal axes were very slightly out of alignment; this, in turn, meant that the measurement probed regions of k space lying slightly off a main symmetry line. Figures 2(a) and 2(b) show projections of the experimental traverse along the k_z, k_x, and k_y axes,[20] while Fig. 2(c) shows a three-dimensional (3D) representation the Brillouin zone for the phase (discussed further below), with the track of the measurement marked. In the photoemission process, only the component of electron momentum parallel to the crystal surface, $k_{\|}$, is conserved upon escaping from the solid. This means that band mapping by ARUPS is straightforward only for two-dimensional systems, a condition approximated to by the cuprate superconductors. In the case of a three-dimensional system, as here, this has the consequence that only the projection of the traverse onto the plane perpendicular to the k_z axis [Fig. 2(a)] is well defined. From this it can be seen that, viewed as a projection along the k_z direction, the experiment probes a line close to, but not coincident with, the Γ-K-X direction. As a result of this, three projections along high-symmetry axes are necessary in order to uniquely specify the traverse in k space. We have chosen the remaining projections to be along k_y and along k_x [Fig. 2(b)]. The projections onto the k_xk_z or k_yk_z planes [Fig. 2(b)] are subject to assumptions about the electron effective mass, and the lattice recoil energy of the crystal. These were chosen to be $m^*=0.65m_e$ (Ref. 21) and $E_{\text{recoil}}=8$ eV,[22] respectively. Many determinations of the electron effective mass for the system with $x=0.2$ are available in the literature. Unfortunately, these vary by an order of magnitude. The value chosen[21] represents a median within the range. As k_z is quite sensitive to the choice of m^*, the projections shown in Fig. 2(b) must be regarded as notional only. Thus, the accuracy of comparison of our results with band-structure calculations is limited by literature uncertainties regarding the electron effective mass. However, the choice of a value substantially less than unity is consistent with values of band mean effective masses obtained for other metallic oxide systems, including the perovskite Na_xWO_3 (Ref. 23) and $Sn_{1-x}Sb_xO_2$.[24]

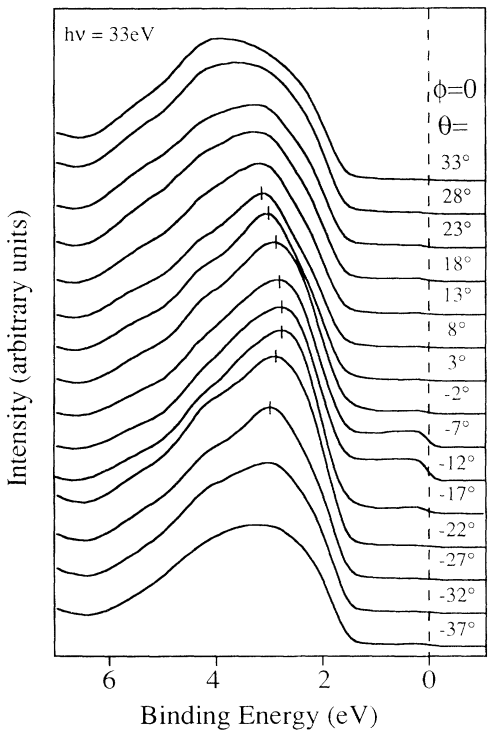

FIG. 1. Angle-resolved EDC's at 33-eV photon energy showing the valence band and Fermi level regions of $BaPb_{0.81}Bi_{0.19}O_3$ (001). Photoelectron emission angles relative to the experimental (chamber) axes are shown. The movement from $\theta=33°$ to $-37°$ corresponds to the k-space traverse shown in Figs. 2(a)–2(c).

The experiment roughly probes an arc of k space which passes through one complete Brillouin zone (BZ) on either side of the Γ point, in a slightly asymmetric traverse, narrowly missing the Γ point itself and other high-symmetry points of the zone. We estimate that the arc reaches the boundaries of the first BZ at points close to L (the midpoint of a hexagonal face of the BZ [Fig. 2(c)]). Close to the Γ point [near normal emission in Fig. 1(a)], the general shape of the valence band (which is composed of O $2p$ and Bi/Pb $6s/p$ hybrids) conforms closely with that seen in angle-integrated measurements.[5,13]

Slight complexities arise in the comparison of our results with linear-augmented-plane-wave (LAPW) band-structure calculations due to the current uncertainty regarding the symmetry of $BaPb_{1-x}Bi_xO_3$ at $x\approx0.2$.[18] The LAPW band-structure calculations of Mattheiss and Hamann[1] follow the assignment of Cox and Sleight,[25] which treats this composition as tetragonal. The electron-diffraction work of Koyama and Ishimaru[26] shows the tetragonal phase at this value of x to be stable to temperatures close to room temperature. Other authors have found the material at this composition to be orthorhombic[3,17] or monoclinic,[19] and our own Laue data suggest an orthorhombic or lower symmetry. In a reexamination of data from the system, Cox and Sleight reached the conclusion that samples having $x\approx0.3$ consisted of mixed orthorhombic and tetragonal phases.[27] They concluded that only the tetragonal phase was superconducting, and that it was stable only at high temperature.[27] Further support for these ideas is found in the work of Asano *et al.*[28] and recent work by Marx *et al.*[18]

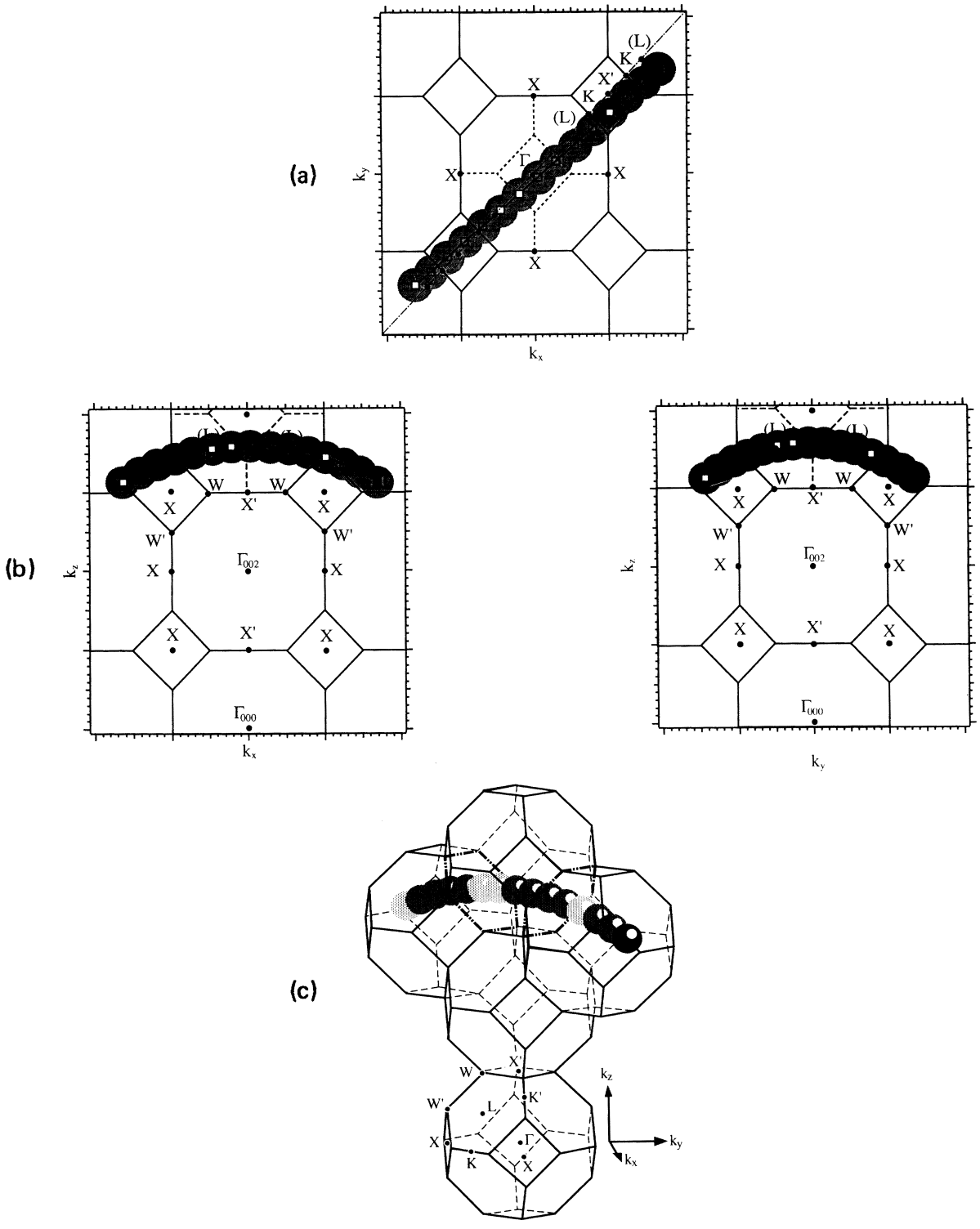

FIG. 2. (a) Projection of the experimental data onto the $k_x k_y$ plane, where the traverse is well defined. The experimental data points are shown by squares, the solid square indicating the analyzer position $\theta=33°$, $\phi=0°$. Open squares show analyzer positions where an enhanced Fermi level DOS is seen, while grey circles indicate the experimental error. Major symmetry points are indicated by solid circles; those shown labeled in brackets do not lie in the $k_x k_y$ plane, and are shown projected onto this plane. (b), (i) and (ii) Projections of the experimental data onto the $k_x k_z$ (i) and $k_y k_z$ (ii) planes, assuming $m^*=0.65m_e$ and $E_{\text{recoil}}=8$ eV (see text). The diagrams use the same notation as (a), and again, major symmetry points not lying in the plane are shown projected onto the plane, and labeled in brackets. The error bars, indicated by grey circles, do not include possible errors in m^* and E_{recoil} (see text). (c) Brillouin zones for the body-centered tetragonal Bravais lattice of $BaPb_{0.8}Bi_{0.2}O_3$, showing the main symmetry points. The track of the experiment is marked. The solid circle tags the analyzer position $\theta=33°$, $\phi=0°$, while the lighter circles indicate analyzer positions where an enhanced Fermi level DOS is seen.

The latter authors conclude that samples in the composition range $0.20 \leq x \leq 0.30$ are disphasic mixtures of tetragonal and orthorhombic phases.[18] Temperature-dependent neutron-diffraction studies of $BaPb_{0.8}Bi_{0.2}O_3$ allow them to observe a structural phase transition from a high-temperature tetragonal (and superconducting) phase to a low-temperature orthorhombic phase, which never proceeds completion as the temperature is lowered.[18] The percentage of tetragonal phase present varies little between 10 K and room temperature; in the region appropriate to our photoemission experiments its value is close to 60%.[18] In the light of our Laue results, it seems possible that the crystal used in the current work may similarly consist of mixed tetragonal and orthorhombic phases at room temperature and below.

In order to compare our results with the band-structure calculation,[1] we have assumed tetragonal symmetry. Fortunately, the effect of any symmetry lowering on the Brillouin zone shape is minimal, though, of course, the size of the irreducible wedge increases as the symmetry is reduced, and in the monoclinic symmetry, L and L' points on adjacent hexagons become distinct from one another. These very slight changes do not produce gross changes in the LAPW calculation,[1] so that comparison with these calculations remains valid.

Band-structure calculations show that the valence-band maximum is expected to be composed of a narrow cluster of nonbonding oxygen states, oriented perpendicular to the nearest-neighbor Pb,Bi bond directions, and lying in the range $\approx 1-2$ eV below E_F. These bands disperse to higher binding energy, and broaden slightly on moving away from Γ. In particular, the downward dispersion on moving from Γ to L or K/K' is of the order of 0.4 eV. In our experiments, the valence-band maximum is observed at rather higher binding energy (around 2.5–3.0 eV below E_F), but a marked dispersion to lower binding energy of the order of 0.3 eV is observed on moving from the Γ point towards the zone edge in either analyzer direction [Fig. 1(a)]. In order to align observed photoemission profiles with calculated LAPW density-of-states (DOS) profiles for oxide materials, it is often found necessary to introduce a rigid downward shift of the complete band structure by an energy of order 1–2 eV.[29] This has generally been attributed to the effects of correlation, which are not explicitly included in the LAPW treatment. With this caveat, the gross features of the valence-band photoemission appear to be in reasonable agreement with the calculated density-of-states profile.[1]

Of particular interest is the DOS at the Fermi energy E_F, and its variation with the analyzer position. Figure 1 shows that this DOS is greatly enhanced at an analyzer position between $\theta = -7°$ and $-12°$. This corresponds to a point in the Brillouin zone away from the Γ point, but close to L [Figs. 2(a) and 2(c)]. Other small enhancements are again seen at $\theta = -37°$ (close to L) and around $\theta = 18°$ (away from a main symmetry point). However, no enhancement is observed at $\theta = 8°$, which is again reasonably close to L, but because of the slightly skewed trajectory, lies between L and W'. Band-structure calculations for the precise composition studied are not available. However, this result appears to be in good general agreement with the LAPW band-structure calculations of Mattheiss and Hamann for $x = 0.3$.[1] These show a widely dispersing Γ_1 band crossing the Fermi energy along the Γ-K'/K and Γ-X/X' directions, and along the Γ-L direction, close to the L point. (Allowing for a rigid 1–2-eV shift of the calculated band structure to high binding energy, the latter crossing would be very close to L.) There is no Fermi level crossing between L and W', which may explain the absence of an enhancement at $\theta = 8°$. The Γ_1 antibonding band is formed by strong $sp\sigma$ interaction between (Pb,Bi) 6s and O 2p orbitals oriented along nearest-neighbor bond directions, and should show predominant (Pb,Bi) 6s character. Resonant photoemission measurements designed to investigate the character of these Fermi level states are in hand.

As discussed above, clear features associated with surface degradation appeared in the valence-band spectra several hours after cleaving, so curtailing the experiment. Difference spectra showed that these new features were centered around 4.4- and 9-eV binding energy, with a small feature around 11.7-eV binding energy. These energies are rather similar to those observed by Kurtz *et al.*[30] on dosing a $La_{1.8}Sr_{0.2}CuO_4$ surface with CO or CO_2, and are characteristic of a surface carbonate-like species.[30] Only two features are observed in the case of a surface hydroxyl species,[30,31] while undissociated H_2O gives three features with rather different relative energies.[31] The appearance of a carbonate-like species is consistent with our earlier observation that $BaCO_3$ is one of the products of extended degradation of this phase.[13,14] This may be formed by adventitious adsorption of CO or CO_2 from the residual vacuum.

We have previously noted the extreme sensitivity of metallic compositions within the $BaPb_{1-x}Bi_xO_3$ system to this type of degradation;[13,14] as x decreases from 1.0, a substantial decrease in stability towards degradation is found at the metal-to-nonmetal transition point ($x \approx 0.4$), with metallic compositions being markedly less stable than nonmetallic compositions.[13,14] This observation may well be linked with the existence of a metastable tetragonal, superconducting phase[18,27] within the metallic composition range; further work is necessary to confirm this suggestion.

In conclusion, ARUPS from $BaPb_{0.81}Bi_{0.19}O_3$ (001) has been measured and compared with LAPW band-structure calculations. Enhancements in the DOS at E_F at points close to L and downward dispersion of the valence-band maximum on moving away from Γ are both in good agreement with calculation. Rapid degradation of the material, resulting in surface carbonate-like species is observed. This behavior may be linked to the metastability of the tetragonal superconducting phase.

This work was supported by the Science and Engineering Council (United Kingdom). We thank Professor D. Cruickshank and Dr. J. Campbell for help with the analysis of the Laue data.

[1]L. F. Mattheiss and D. R. Hamann, Phys. Rev. B **28**, 4227 (1983).
[2]A. W. Sleight, J. L. Gillson, and B. E. Bierstedt, Solid State Commun. **17**, 27 (1975).
[3]Y. Khan, K. Nahm, M. Rosenberg, and H. Willner, Phys. Status Solidi A **39**, 79 (1977).
[4]See, e.g., J. Yu, X. Y. Chen, and W. P. Su, Phys. Rev. B **41**, 344 (1990); D. Nguyen Manh, D. Mayou, and F. Cyrot-Lackmann, Europhys. Lett. **13**, 167 (1990).
[5]H. Matsuyama, T. Takahashi, H. Katayama-Yoshida, Y. Okabe, H. Takagi, and S. Uchida, Phys. Rev. B **40**, 2658 (1989).
[6]M. Nagoshi, Y. Fukuda, T. Suzuki, K. Ueki, A. Tokiwa, M. Kikuchi, Y. Syono, and M. Tachiki, Physica C **185-189**, 1051 (1991).
[7]H. Matsuyama, T. Takahashi, H. Katayama-Yoshida, Y. Okabe, H. Takagi, and S. Uchida, Physica C **162-164**, 1319 (1989).
[8]C. L. Lin, S. L. Qiu, J. Chen, M. Strongin, G. Cao, C-S. Jee, and J. E. Crow, Physica C **39**, 9607 (1989).
[9]A. Winiarski, G. Wübbeler, Chr. Scharfschwerdt, E. Clausing, and M. Neumann, Fresenius J. Anal. Chem. **341**, 296 (1991).
[10]M. Nagoshi, T. Suzuki, Y. Fukuda, A. Tokiwa-Yamamoto, Y. Syono, and M. Tachiki, Phys. Rev. B **47**, 5196 (1993).
[11]A. Fujimori, J. Phys. Chem. Solids **53**, 1595 (1992).
[12]H. Guyot, Cl. Filippini, and J. Marcus, J. Alloys Compounds **195**, 543 (1993).
[13]W. R. Flavell, A. J. Roberts, B. C. Morris, D. R. C. Hoad, I. Tweddell, A. Neklesa, R. Lindsay, G. Thornton, P. L. Wincott, and T. S. Turner, Supercond. Sci. Technol. **5**, 648 (1992).
[14]W. R. Flavell, D. R. C. Hoad, A. J. Roberts, R. G. Egdell, I. W. Fletcher, and G. Beamson, J. Alloys Compounds **195**, 535 (1993).
[15]M. Nagoshi, T. Suzuki, Y. Fukuda, K. Ueki, A. Tokiwa, M. Kikichi, Y. Syono, and M. Tachiki, J. Phys. Condens. Matter **4**, 5769 (1992).
[16]B. M. Wanklyn, Chen Changkang, and J. W. Hodby, J. Less-Common Met. **164-165**, 926 (1990).
[17]M. Oda, Y. Hidaka, A. Katsui, and T. Murakami, Solid State Commun. **55**, 423 (1985).
[18]D. T. Marx, P. G. Radaelli, J. D. Jorgensen, R. L. Hitterman, D. G. Hinks, S. Pei, and B. Dabrowski, Phys. Rev. B **46**, 1144 (1992).
[19]J. Ihringer, J. K. Maichle, W. Prandl, A. W. Hewat, and T. Wroblewski, Z. Phys. B **82**, 171 (1991).
[20]This trajectory, which does not pass directly along high symmetry directions, is calculated using a procedure outlined in M. Mian and W. R. Flavell (unpublished).
[21]S. Tajima, K. Kitazawa, and S. Tanaka, Solid State Commun. **47**, 659 (1983).
[22]R. Courths and S. Hüfner, Phys. Rep. **112**, 91 (1984).
[23]M. D. Hill and R. G. Egdell, J. Phys. C **16**, 6205 (1983).
[24]R. G. Egdell, W. R. Flavell, and P. Tavener, J. Solid State Chem. **51**, 345 (1984).
[25]D. E. Cox and A. W. Sleight, in *Proceedings of Conference on Neutron Scattering*, Gatlinberg, Tennessee, 1976, edited by R. M. Moon (National Technical Information Service, Springfield, VA, 1976).
[26]Y. Koyama and M. Ishimaru, Phys. Rev. B **45**, 9966 (1992).
[27]A. W. Sleight and D. E. Cox, Solid State Commun. **58**, 347 (1986).
[28]H. Asano, M. Oda, Y. Endoh, Y. Hidaka, F. Izumi, T. Ishigaki, K. Karahashi, T. Murakami, and N. Watanabe, Jpn. J. Appl. Phys. **27**, 1638 (1988).
[29]See, e.g., R. G. Egdell, W. R. Flavell, and M. S. Golden, Supercond. Sci. Technol. **3**, 8 (1990).
[30]R. L. Kurtz, R. Stockbauer, T. E. Madey, D. Mueller, A. Shih, and L. Toth, Phys. Rev. B **37**, 7936 (1988).
[31]W. R. Flavell, J. H. Laverty, D. S.-L. Law, R. Lindsay, C. A. Muryn, C. F. J. Flipse, G. N. Raiker, P. L. Wincott, and G. Thornton, Phys. Rev. B **41**, 11 623 (1990).

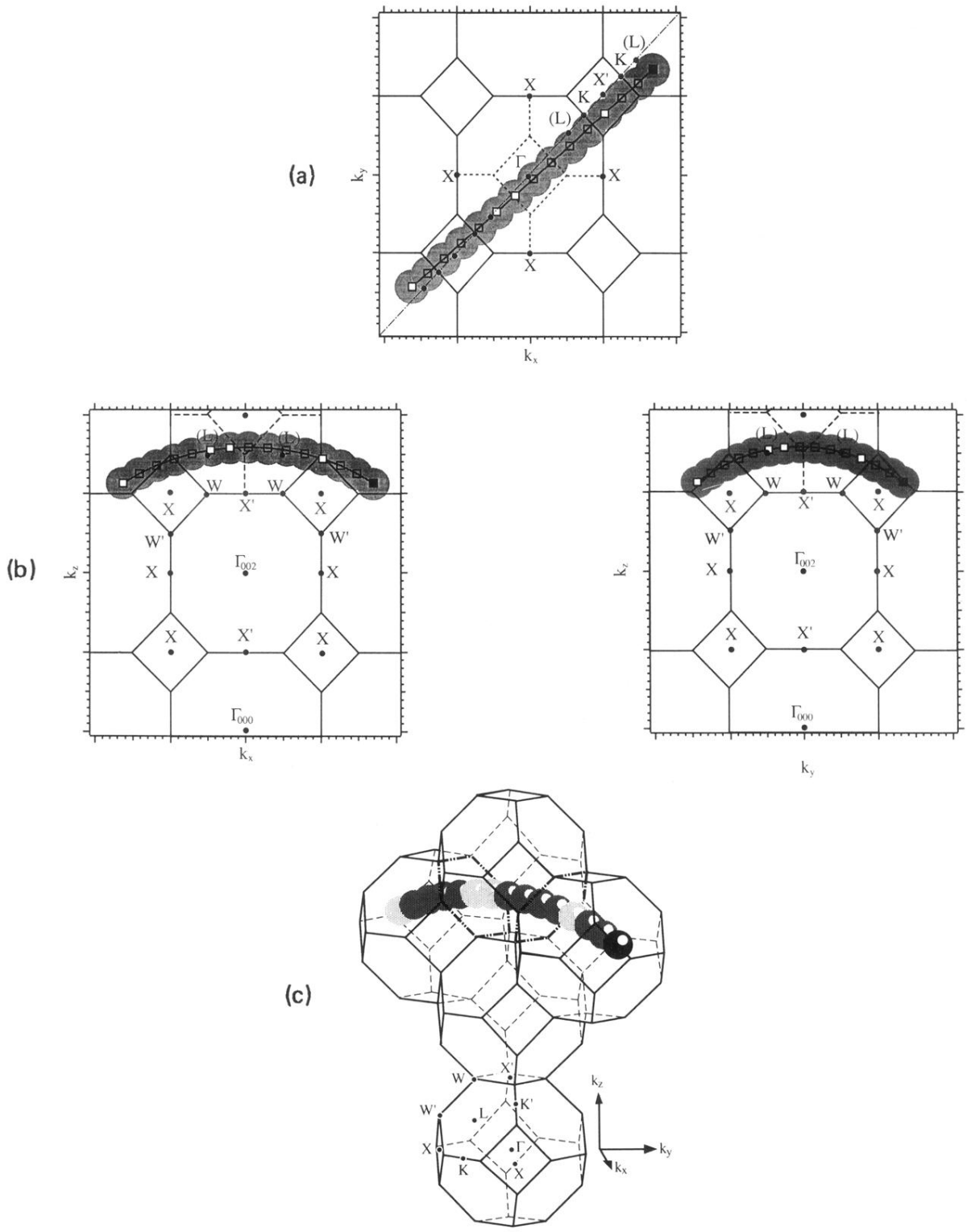

FIG. 2. (a) Projection of the experimental data onto the $k_x k_y$ plane, where the traverse is well defined. The experimental data points are shown by squares, the solid square indicating the analyzer position $\theta=33°$, $\phi=0°$. Open squares show analyzer positions where an enhanced Fermi level DOS is seen, while grey circles indicate the experimental error. Major symmetry points are indicated by solid circles; those shown labeled in brackets do not lie in the $k_x k_y$ plane, and are shown projected onto this plane. (b), (i) and (ii) Projections of the experimental data onto the $k_x k_z$ (i) and $k_y k_z$ (ii) planes, assuming $m^*=0.65m_e$ and $E_{\text{recoil}}=8$ eV (see text). The diagrams use the same notation as (a), and again, major symmetry points not lying in the plane are shown projected onto the plane, and labeled in brackets. The error bars, indicated by grey circles, do not include possible errors in m^* and E_{recoil} (see text). (c) Brillouin zones for the body-centered tetragonal Bravais lattice of $BaPb_{0.8}Bi_{0.2}O_3$, showing the main symmetry points. The track of the experiment is marked. The solid circle tags the analyzer position $\theta=33°$, $\phi=0°$, while the lighter circles indicate analyzer positions where an enhanced Fermi level DOS is seen.